PHILOSOPHICAL TRANSACTIONS OF THE ROYAL SOCIETY A MATHEMATICAL, PHYSICAL & ENGINEERING SCIENCES

Dynamics of Scroll Waves in Inhomogeneous Excitable Media

Arkady Pertsov and Michael Vinson

Phil. Trans. R. Soc. Lond. A 1994 **347**, 687-701
doi: 10.1098/rsta.1994.0075

Dynamics of scroll waves in inhomogeneous excitable media†

By Arkady Pertsov[1] and Michael Vinson[2]‡

[1]*Institute of Experimental and Theoretical Biophysics, Pushchino, Moscow Region 142292, Russia and Department of Pharmacology, SUNY Health Sciences Center, Syracuse, New York 13210, U.S.A.*

[2]*Department of Physics, and Northeast Parallel Architectures Center, Syracuse University, Syracuse, New York 13244, U.S.A.*

Nonlinear waves in excitable media often organize themselves into vortex-like patterns of activity, called 'scroll waves' in three dimensions. In this paper we review recent results concerning the effects of inhomogeneities on scroll wave dynamics. We concentrate on the dynamics of scroll waves with initially rectilinear filaments evolving in the presence of linear parameter gradients with different orientations relative to the filament. We describe how this evolution is affected by the presence of localized defects. The effects described here are important in the study of cardiac arrhythmias, and may lead to an understanding of the mechanism of termination and stabilization of these arrhythmias.

1. Introduction

Nonlinear waves in excitable media often organize themselves into vortex-like patterns of activity (for reviews, see Krinsky 1984; Winfree 1990; Swinney & Krinsky 1991; Keener 1992). These vortices have been studied in chemical reactions (Zhabotinsky & Zaikin 1971; Winfree 1972) and biological systems such as electrochemical propagation in myocardial tissue (Davidenko *et al.* 1992), aggregation of slime-molds (Gerisch 1965; Siegert & Weijer 1991), spreading depression waves in the brain and retina (Gorelova & Bures 1983), and elsewhere (Lechleiter *et al.* 1991). In the case of myocardial tissue, these vortices are thought to underlie pathological high frequency rhythms of the heart (Pertsov *et al.* 1993*a*).

These vortices, called 'spiral waves' in two dimensions and 'scroll waves' in three dimensions, are described by the phase singularity at the centre of the vortex. This singularity is a point in two dimensions, and a curve in three dimensions, called the 'filament' (Winfree & Strogatz 1984; Panfilov & Pertsov 1984). Figure 1 shows examples of scroll waves in homogeneous media, from computer simulation (*a*) and Belousov–Zhabotinskii (BZ) reaction (*b*). In both cases, the filament is a straight line, oriented in the z direction, and the wave rotates around the filament

† This paper was produced from the authors' disk by using the TEX typesetting system.

‡ Present address: Department of Physics, Shippensburg University, Shippensburg, Pennsylvania 17257, U.S.A.

Phil. Trans. R. Soc. Lond. A (1994) **347**, 687–701
Printed in Great Britain

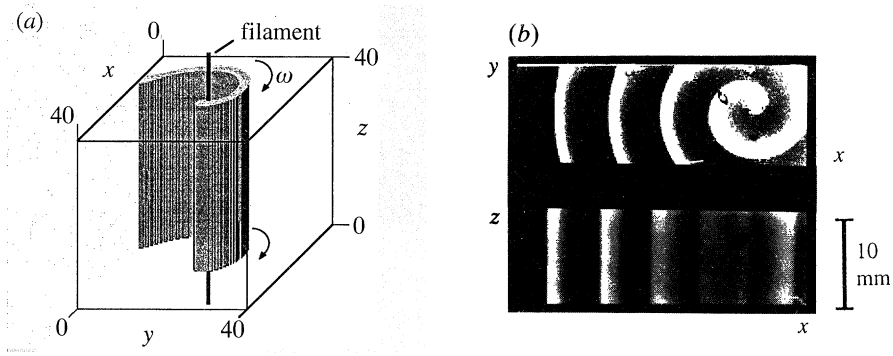

Figure 1. Scroll wave with straight-line filament. (*a*) From the computer simulation of FitzHugh–Nagumo model. The activated (excited) regions are shown in dark gray. The filament is the phase singularity around which the scroll rotates, shown as a heavy dark line. Arrows show the direction of rotation of the scroll; the scroll rotates with angular frequency ω. (*b*) Two projections of a scroll wave in BZ reaction. In the (x, y) projection, the scroll appears as a spiral; in the (x, z) projection, the wave appears as a set of planar waves.

in a clockwise sense. A filament of this type (straight line, perpendicular to the boundaries of a homogeneous medium) is stationary. There is a translational symmetry along the filament; each slice of a scroll wave perpendicular to the z direction contains an identical two-dimensional spiral wave.

When the filament is not straight or when the medium is not homogeneous, the scroll wave in general is no longer stationary. Its motion is determined by the geometry of the filament (intrinsic) and the effects of the inhomogeneities of the medium (extrinsic). The complicated motion of such a vortex in a three-dimensional medium may be decomposed into the rapid rotation of the vortex around the filament and the slow movement of the filament through space (Winfree 1973; Panfilov & Pertsov 1984; Jahnke *et al.* 1988; Keener & Tyson 1992).

Experimental observations of vortices in autocatalytic chemical reactions and myocardial tissue have demonstrated the significant effect of heterogeneities on the motion of the vortex wave. These effects include drift and twisting of vortices due to parameter gradients (Skinner & Swinney 1991; Aliev & Rovinsky 1992; Davidenko *et al.* 1992; Fast & Pertsov 1992; Steinbock *et al.* 1992; Braune & Engel 1992; Siegert *et al.* 1992; Agladze & de Kepper 1992; Pertsov *et al.* 1993*a*; Pertsov *et al.* 1990; Yamaguchi & Müller 1991). Heterogeneities in the form of localized defects have been shown to lead to the anchoring of vortices (Davidenko *et al.* 1992; Nettesheim *et al.* 1992; Pertsov *et al.* 1993*a*). In the case of the heart, drift and anchoring of vortices can lead respectively to termination and stabilization of dangerous arrhythmias, and thus their study is important from a practical standpoint (Davidenko *et al.* 1992; Pertsov *et al.* 1993*a*).

Until recently, analysis of inhomogeneous excitable media has been limited to two dimensions. The analysis of vortices in three dimensions has mainly focused on the intrinsic motion of scroll waves in homogeneous media (for reviews see Winfree 1990; Keener & Tyson 1992), whereas the study of three-dimensional inhomogeneous media is still in its infancy. In this paper we review recent results concerning the effects of inhomogeneities on scroll wave dynamics in three dimensions. We will concentrate on the dynamics of scroll waves with initially rectilinear filaments evolving in the presence of linear parameter gradients with

PHILOSOPHICAL TRANSACTIONS OF THE ROYAL SOCIETY A MATHEMATICAL, PHYSICAL & ENGINEERING SCIENCES

different orientations relative to the filament. We will describe how this evolution is affected by the presence of localized defects.

The data discussed in this paper are mainly based on computer simulations of the modified FitzHugh–Nagumo equation, a nonlinear reaction-diffusion equation:

$$\frac{\partial \boldsymbol{u}}{\partial t} = \boldsymbol{f}(\boldsymbol{u}) + \boldsymbol{D}\boldsymbol{u}, \tag{1.1}$$

where $\boldsymbol{D}$ is a diffusion matrix and $\boldsymbol{f}(\boldsymbol{u})$ is a nonlinear function of $\boldsymbol{u}$. The particular model used here is given by:

$$\frac{\partial E(\boldsymbol{x},t)}{\partial t} = f(E(\boldsymbol{x},t)) - g(\boldsymbol{x},t) + D\nabla^2 E(\boldsymbol{x},t) + \gamma(\boldsymbol{x}), \tag{1.2}$$

$$\frac{\partial g(\boldsymbol{x},t)}{\partial t} = (E(\boldsymbol{x},t) - g(\boldsymbol{x},t))/\tau(E(\boldsymbol{x},t),\boldsymbol{x}). \tag{1.3}$$

Here E is the excitation of the medium; g is the recovery. The term $\gamma(\boldsymbol{x})$ provides an inhomogeneity in the excitation threshold. For example, if $\gamma(\boldsymbol{x}) = (x - x_0)\alpha$, then there is a smooth linear gradient in the x direction, with strength of the gradient controlled by α. The dependence of τ on $\boldsymbol{x}$ is used to introduce a localized inhomogeneity. As usual, zero flux boundary conditions for E and g are imposed on the boundaries of the medium. Equations (1.2) and (1.3) are often used in studies of excitable media, in particular in simple models of excitation propagation in cardiac tissue (Pertsov *et al.* 1993*a*). The appendix gives details of the model and parameters used in the simulations described below.

The paper is organized as follows. In § 2, we consider the effects of a smooth parameter gradient without localized defects; we consider two basic cases: one in which the gradient is parallel to the filament (§ 2*a*), and one in which it is perpendicular to the filament (§ 2*b*). In § 3, we discuss the effect of a localized defect on a scroll wave drifting in a smooth parameter gradient. We conclude (§ 4) with a discussion of the present limitations and future directions in the study of three-dimensional inhomogeneous media.

2. Smooth inhomogeneities

(*a*) *Gradient perpendicular to the filament: drift*

We begin with a simple scroll wave with a straight line filament, oriented perpendicular to a linear parameter gradient (with no localized defect). Computer simulations show that in this case the filament drifts as a straight line without deformation, and is stable to small perturbations (Vinson *et al.* 1993). Figure 2*a*, *b* shows three-dimensional views of such a filament, drifting due to the parameter gradient along the x-axis. As the filament drifts, its speed increases, as can be seen from the distance between successive filaments in figure 2*b*. The vortex continues to drift until it encounters the boundary of the medium and annihilates. Figure 2*c* shows the (x, y) projection of the time evolution of the filament (heavy black line) and the tip of the spiral wave (thin line). The trajectory of the tip follows a cycloidal motion with a net drift both parallel to and perpendicular to the gradient.

A drifting vortex in myocardial tissue is illustrated in figure 3. Figure 3*a* shows a snapshot of the vortex, with excited regions shown in white. The characteristic

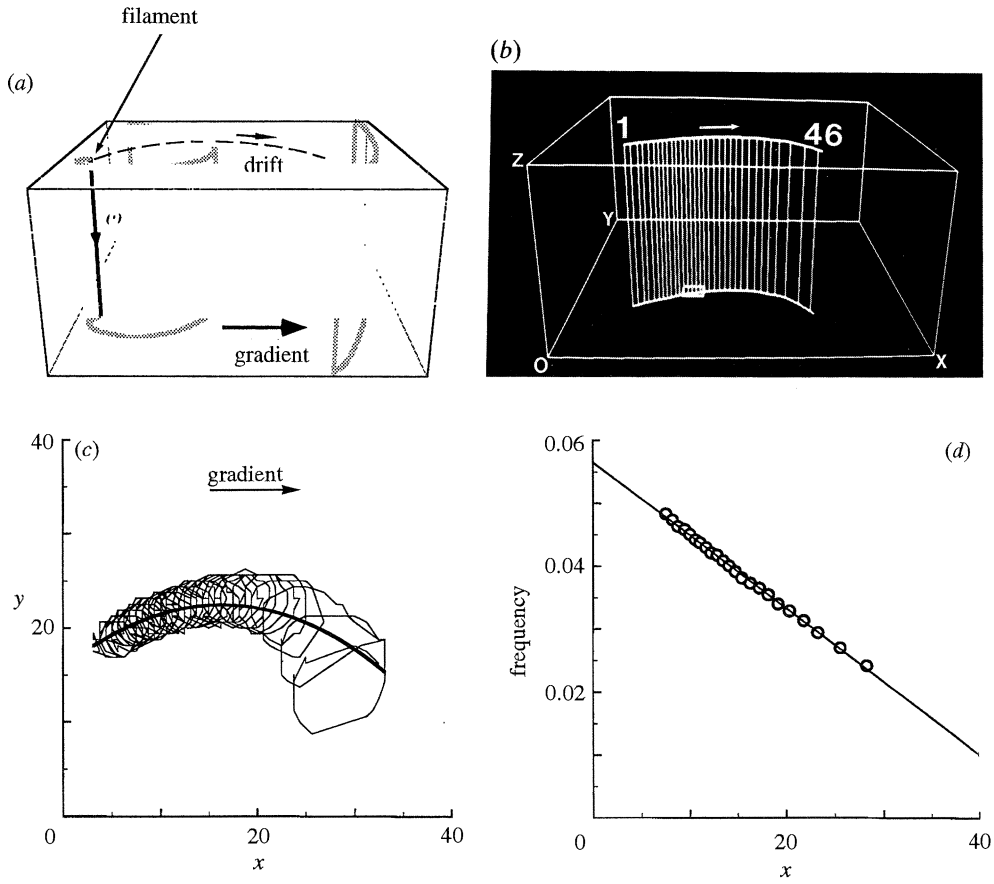

Figure 2. Drift of a simple scroll wave in parameter gradient perpendicular to the filament. (*a*) Schematic of the scroll wave, showing the filament (dark line) and wave-front (gray curves). The gradient is oriented to the right (the $+x$ direction). (*b*) Successive snapshots of the drifting filament, from computer simulation. The filament remains straight, and executes an approximately parabolic trajectory. 46 rotation periods are shown. (*c*) Two-dimensional projection showing trajectories of the filament in the (x, y) plane (thick line) and of the scroll wave tip (thin line). The tip is determined by the intersection of lines of iso-E and iso-g (at values of 0.5 each). The tip traces out the boundary of the core of the scroll wave; the centre of mass points over each rotation of the scroll are taken to be the locations of the filament. (*d*) Scroll wave frequency as a function of x position. The line is from linear regression. The scroll drifts toward the region of lower frequency. (Adapted from Vinson *et al.* 1993.)

spiral shape can clearly be seen. The velocity of the drifting can be directly measured from the slope of the line through the centre of the branching pattern in the time–space plot shown in figure 3*b* (Pertsov *et al.* 1993*b*). The spiral drifts to the right due to intrinsic gradients in the tissue sample.

Generally as a scroll wave drifts, its frequency of rotation decreases. The dependence of the rotation frequency on the position of the filament is shown in figure 2*d*, from computer simulation. The rotation frequency decreases almost linearly with x. The drift toward lower frequency is consistent with data obtained in two-dimensional media with other types of gradients (Rudenko & Panfilov 1983; Pertsov & Ermakova 1988; Zou *et al.* 1993). In this regard, it is tempting to make

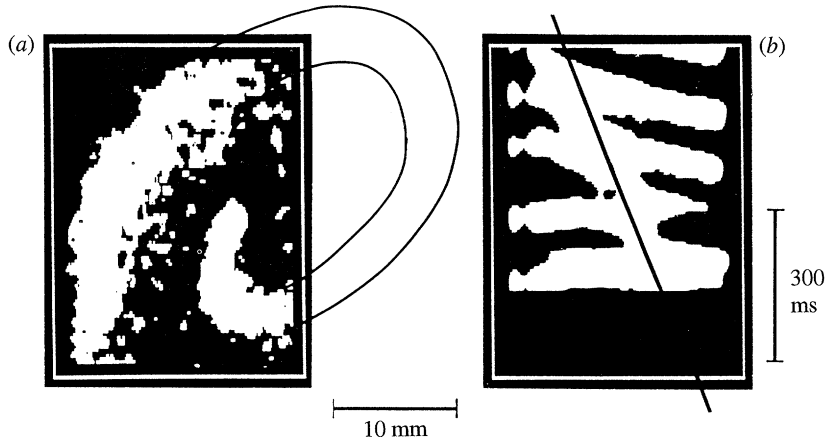

Figure 3. Drift of a spiral wave in myocardium. (*a*) Snapshot of the spiral wave. The excited areas are shown in white. Only the central part of the spiral can be seen. Lines have been added to indicate how more of the spiral would appear if the medium were larger. (*b*) Time–space plot (Davidenko *et al.* 1992; Pertsov *et al.* 1993*b*), showing the drift of the spiral. The vertical coordinate is time, horizontal is x. The branches correspond to projections of the propagating wave, and the branching region corresponds to the phase singularity at the centre of the spiral. The branching region shifts to the right, indicating the drift of the spiral. (Adapted from Pertsov *et al.* 1993*a*.)

an analogy between a vortex drifting in a parameter gradient and a particle moving in a potential field with dissipation. The motion of the particle takes it to the region of lower energy; in the case of the vortex it moves to the region of lower frequency, where the dissipation of energy is lower.

In addition to the drift parallel to the gradient, there is also a component of drift perpendicular to it. This perpendicular component is in opposite directions for scrolls rotating in the clockwise and counter-clockwise directions. This component of the drift velocity depends on the excitability of the medium; as can be seen in figure 2, this component changes sign, giving rise to the parabolic trajectory. Because the sign of this component depends on the sense of rotation of the scroll, it can be used to study the collision of scroll (or spiral) waves (Rudenko & Panfilov 1983; Schütze *et al.* 1992).

It should be noted that the straight-line filament perpendicular to the parameter gradient is stable to symmetry-breaking perturbations. The scroll drifts without deformation of the filament and preserves the translational symmetry along the filament. This observation makes it possible to consider this case as quasi-two-dimensional, and the phenomenology of drift in two-dimensional systems (Rudenko & Panfilov 1983; Pertsov & Ermakova 1988) can be applied.

(*b*) *Gradient parallel to the filament: twist*

When the gradient is parallel to the filament there is no longer a translational symmetry along the filament, and instead of a drifting scroll wave, a different structure emerges: a twisted scroll wave. Twisted scroll waves were predictied from topological analysis by Winfree & Strogatz (1984). In homogeneous media, twisted scrolls have been shown to be unstable; a twisted scroll untwists and leads to a simple scroll wave (Panfilov *et al.* 1984; Biktashev 1989; Pertsov *et al.* 1990).

PHILOSOPHICAL TRANSACTIONS OF THE ROYAL SOCIETY A MATHEMATICAL, PHYSICAL & ENGINEERING SCIENCES

This is not the case in inhomogeneous media, in which a twisted scroll wave may be stable, and can evolve from an untwisted scroll.

Figure 4 shows a twisted scroll wave that emerged due to a gradient oriented parallel to the initial filament. Although the wave front appears quite complicated, it is nothing but a simple twisted scroll with a straight-line filament. Indeed, each cross-section perpendicular to the filament contains a simple spiral wave, as shown in figure 4*b*. The phase of these spirals shifts as the filament is traversed from top to bottom. Figure 4*b* shows three such cross-sections; the one in the middle has a phase shift of $\Delta\phi = \pi$ relative to the top, and bottom slice is shifted π further. The twist is the amount by which the phase of the spiral differs from cross-section to cross-section. By definition, the twist w is $\mathrm{d}\phi(s)/\mathrm{d}s$, where $\phi(s)$ is the phase of the spiral wave in the cross-section at location s along the filament. (For the rectilinear filament of figure 4, the coordinate s is just z.) As shown in figure 4*c*, a cross section of the wavefront containing the filament yields a characteristic 'fir tree' pattern. The twist can be obtained from the wavelength (λ) and the distance along the filament over which the phase shifts by 2π (ℓ) via $w = 2\pi\lambda/\ell$. This formula is used to compute twist of scrolls in BZ reaction experiments (Pertsov *et al.* 1990).

The mechanism of twist formation is a result of the natural frequency of rotation being different for different points along the filament, due to the parameter gradient (Pertsov *et al.* 1990; Panfilov *et al.* 1984). Considering two points on the filament with local natural rotation frequencies ω_1 and ω_2, one expects the phase difference between the points initially to grow linearly in time as $\Delta\phi = (\omega_2 - \omega_1)t$. This differential rotation causes the development of twist.

The phase difference cannot grow indefinitely, however. If the gradient is not too large, the twist reaches an equilibrium value. The larger the gradient, the larger the equilibrium twist. The mechanism of equilibration involves the acceleration of the slower part of the filament, resulting in a stable twisted scroll rotating at the faster rate (Mikhailov *et al.* 1985; Panfilov *et al.* 1984). Figure 5 shows a twisted scroll in a BZ reaction. The container initially has a temperature gradient in the vertical direction; the scroll labelled A-B is clearly twisted, as can be seen from its conic shape (cf. figure 4).

In contrast to heterogeneous media, homogeneous media cannot support stable twisted scrolls (Pertsov *et al.* 1990; Panfilov *et al.* 1984). The twist of an initially twisted scroll wave decays in time, leading to a simple untwisted scroll. This has been demonstrated, first in computer simulations (Panfilov *et al.* 1984), then in experiments with the BZ reaction (Pertsov *et al.* 1990). Figure 5*b* shows the effect of untwisting in BZ reaction. After the temperature gradient has been removed, the twist is less, as can be seen from the wave front being almost parallel to filament A-B.

If the gradient exceeds a critical value, the twist does not equilibrate; strong gradients inevitably lead to breakdown of the scroll and the formation of a complicated, turbulent-like state. This phenomenon has been observed both experimentally (in BZ reaction (Pertsov *et al.* 1990)) and in computer simulations (Panfilov 1993). There are two different hypotheses to account for this breakdown. First, the frequency of rotation may continue to increase due to the formation of twist until it reaches the highest frequency the medium can support. When this occurs, any heterogeneities in the medium will produce multiple wave breaks, leading to proliferation of disorganized filaments which then evolve and interact. The sec-

PHILOSOPHICAL TRANSACTIONS OF THE ROYAL SOCIETY A MATHEMATICAL, PHYSICAL & ENGINEERING SCIENCES

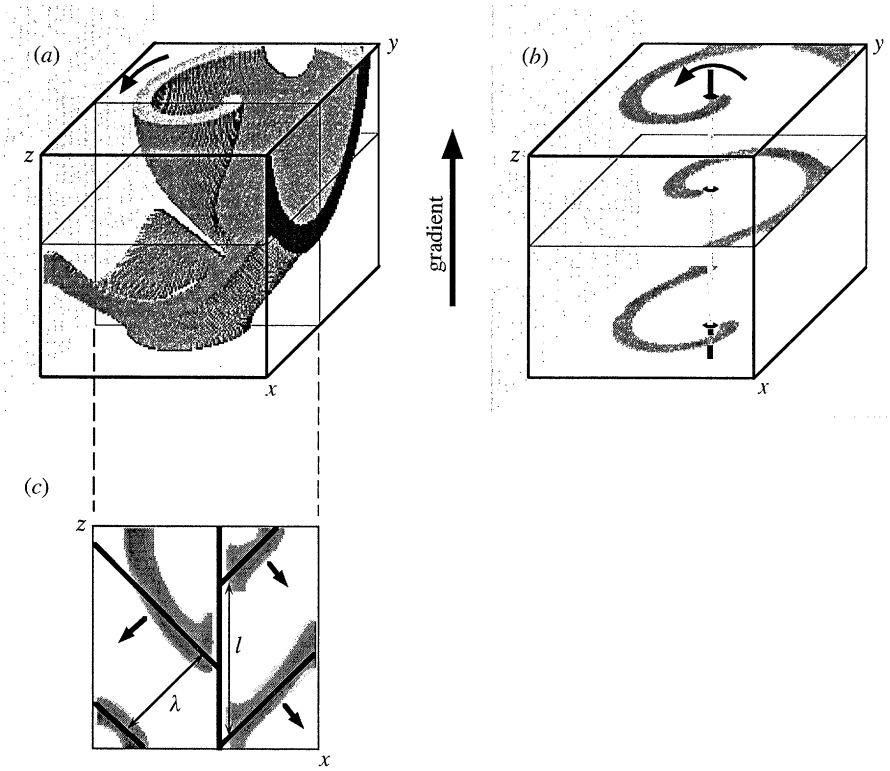

Figure 4. Twisted scroll wave in parameter gradient parallel to the filament. (*a*) Equilibrium twisted scroll from FitzHugh–Nagumo computer simulation. The conic structure is typical of a twisted scroll. (*b*) Three horizontal cross sections of the scroll in part (*a*), showing the spiral structure. The filament is shown as a gray line. (*c*) A vertical cross section of the twisted scroll through the filament, demonstrating the specific branching structure indicative of twist. Arrows show the direction of propagation. The central vertical line is the filament, the branching lines follow the wave fronts. λ is the wavelength of the scroll, and ℓ is the distance over which the phase shift is 2π. The twist is then $w = 2\pi/\ell$.

ond hypotheses, based on recent observations of computer simulations, is that the initially straight filament can rapidly 'sproing' into a helical shape (Henze *et al.* 1990). In a bounded medium, the expanding helical filament may collide with the borders, leading again to multiple disorganized vortices. It is unclear whether 'sproinging' is a critical phenomenon, or whether the helical shape grows smoothly with the degree of twist.

The formation of twist and the breakdown of twisted scrolls is likely to be important in cardiac arrhythmias. Cardiac tissue has smooth heterogeneities through the thickness of the myocardial wall (see Liu *et al.* 1993). These heterogeneities have been observed to increase in certain pathological conditions. A scroll wave oriented along a heterogeneity will, as discussed above, become twisted. If the heterogeneity is sufficiently strong, the twist will eventually exceed the critical value, and the scroll will break down, as seen in the BZ reaction (Pertsov *et al.* 1990). The break down into multiple disorganized vortices, if it occurs in the heart, would lead to a phenomenon similar to fibrillation, which is associated with sudden cardiac death.

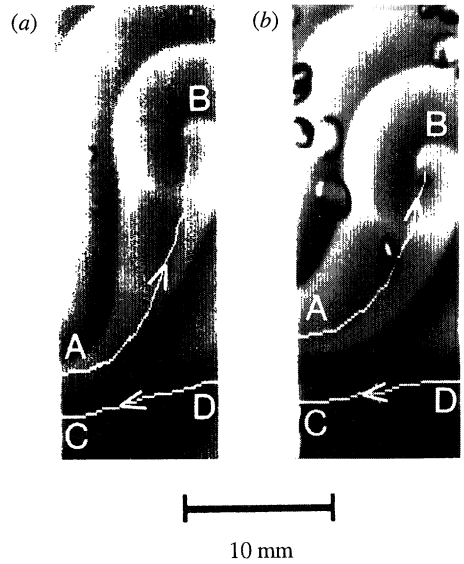

Figure 5. Snapshots of twisted scroll waves from BZ reaction experiment. Front view. The white lines show the positions of the filaments, with arrows indicating sense of rotation. (*a*) Scroll waves shortly after initiation. Filament A-B is significantly twisted, as can be seen from the characteristic conical shape of the wave front (compare figure 4). The twist is due to a temperature gradient in the vertical direction. Horizontally oriented filament C-D is less twisted because its projection in the direction of the gradient is small. (*b*) The same scroll waves one hour later (30 min after removal of gradient). The filaments became shorter and show a smaller degree of twist. Figure from Pertsov *et al.* (unpublished data).

3. Localized inhomogeneities

(*a*) *Anchoring of filaments*

We now consider the effect of a localized inhomogeneity or defect on a scroll wave drifting in a parameter gradient. In two dimensions, it has been shown that when the trajectory of the singularity brings it sufficiently close to the defect, it moves toward the defect until it attaches to it. Once anchored, it remains so indefinitely. When the singularity is far enough from the obstacle that it does not fall within its basin of attraction, the spiral wave drifts without anchoring (Davidenko *et al.* 1992; Vinson *et al.* 1993; Zou *et al.* 1993).

Anchoring of vortices may also occur in three dimensions, but with some significant differences (Vinson *et al.* 1993). In three dimensions, only part of the filament is attracted to the defect; the part of the filament that is not attracted to the defect continues to evolve. There is thus a competition between the anchored end of the filament and the free end. This competition produces qualitatively different dynamics in three dimensions. For larger defects, anchoring still takes place but with a timescale of equilibration several orders of magnitude larger than in the two-dimensional case. Below a critical height, equilibration does not occur; a new phenomenon, temporary anchoring, appears instead.

The phenomenon of anchoring in a three-dimensional case is depicted in figure 6. Here the defect height is one-quarter the height of the medium, and initial conditions are such that the trajectory of the filament passes through the position

of the defect. Figure 6*a* shows the filament at successive instants of time. As expected from the two-dimensional case, the lower portion of the filament is attracted by and anchors to the defect. However, the upper portion continues to drift. The trajectory of the top begins to curl around, rotating about the defect (where the lower portion of the filament is anchored) until it reaches an equilibrium after approximately 60 rotation periods. Throughout the anchoring process, the filament remains approximately planar. Figure 6*b* shows a snapshot of the equilibrated scroll wave.

The equilibration in three dimensions is much slower than in two dimensions. In the latter case, a drifting scroll encounters an obstacle and anchors to it very rapidly, in two or three rotation periods (Pertsov *et al.* 1993*a*; Vinson *et al.* 1993; Zou *et al.* 1993). In three dimensions, however, as discussed above the equilibration can take 60 rotation periods, about 20 times longer than in two dimensions. The difference between the two cases becomes less when the height of the defect is increased; a larger obstacle attracts more of the filament, and the free part equilibrates more rapidly.

Figure 6*c* shows the rotation frequency of the scroll wave as a function of time with and without a defect. Up to time equal to 500, the rotation frequency with the defect follows the case without; however, for later times, the curves diverge. Without the defect, the frequency continues to decrease as the spiral continues to drift, whereas with the defect, the frequency reaches a minimum value and then slowly increases towards equilibrium. The equilibration time is on the order of 2000 (which corresponds to approximately 60 rotation periods).

Anchoring generally leads to filament twist (Vinson *et al.* 1993). There are two mechanisms contributing to the appearance of twist. The first is a consequence of the anchored filament having a projection parallel to the direction of the gradient, leading to twist as discussed in § 2*a*. The second mechanism is due to the perturbation of the natural rotation frequency by the defect at the anchored end; as a rule this effect decreases the natural frequency of the anchored part of the filament (Vinson *et al.* 1993; Zou *et al.* 1993). Figure 6*b* shows a snapshot of an anchored scroll wave. The cone-shaped structure characteristic of a twisted scroll can be seen. The twist of this scroll wave is such that the top has a phase advance relative to the bottom, implying that the natural rotation frequency of the top is higher. Thus although the top of the scroll is located in a region of lower frequency, the second mechanism causes the bottom of the scroll to lag behind.

Note that in this paper we do not consider the role of a localized defect in the presence of a gradient parallel to the filament. In this case, there is no drift and therefore anchoring as such does not occur. The defect can, however, perturb the twist of the scroll wave. When the obstacle is located away from the core region of the scroll, it has no significant effect on the evolution of the wave. When it is located near the filament, it may reduce the twist or increase it, depending upon the size of the defect, its position along the filament, and its shape and other properties. In contrast to the case of drift and anchoring discussed here, the phenomena that occur when the gradient is parallel to the filament do not yield generic results, but depend on details of the system.

(*b*) *Detachment of filaments*

There is another major difference between two- and three-dimensional filament dynamics in the presence of a localized defect. In two dimensions, the filament

PHILOSOPHICAL TRANSACTIONS OF THE ROYAL SOCIETY A MATHEMATICAL, PHYSICAL & ENGINEERING SCIENCES

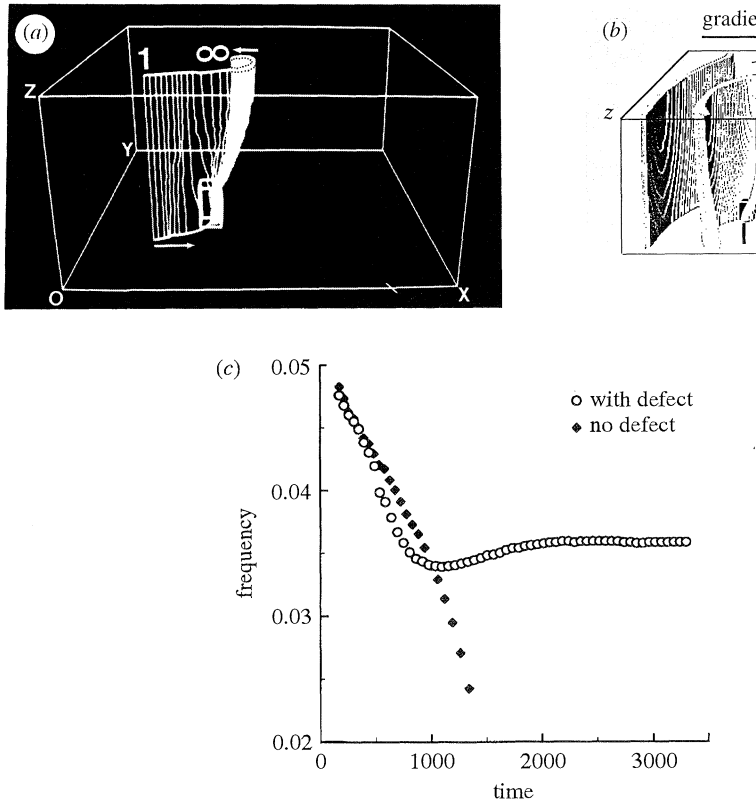

Figure 6. Anchoring of a scroll wave to a localized defect. (*a*) Successive snapshots of the filament during the anchoring process. The parameter gradient is to the right ($+x$ direction). Parameters as in figure 2, with the addition of a localized defect. (*b*) Snapshot of anchored scroll wave. The effect of twist can be seen in the conic shape of the wave front (cf. figure 4). (*c*) Rotation frequency versus time with and without the defect. (Adapted from Vinson *et al.* 1993.)

either anchors to the defect, or it misses the defect completely (Davidenko *et al.* 1992; Zou *et al.* 1993). In three dimensions, an intermediate phenomenon, temporary attachment, can occur (Vinson *et al.* 1993; Zou *et al.* 1993). If the height of the defect is lower than a critical height, then although the filament initially anchors, after a time it pulls free, or detaches, from the defect. Following detachment, the filament executes a complicated rotary, 'spring-like' motion.

The phenomenon of detachment is illustrated in figure 7. The defect height is 10% less than that needed to cause anchoring (figure 6). As in the anchoring case, one end of the filament is attracted by the defect and attaches to it, and for the first 44 rotation periods there is a tendency towards stabilization. During this time, the motion is virtually identical to that of figure 6; in particular, the bottom of the filament is rapidly attracted to the defect, and the top end begins to rotate about the base. After approximately 44 rotation periods, however, the lower portion of the filament pulls free from the defect.

Figure 7*b* shows how the rotation frequency as a function of time changes during detachment. Initially, the frequency during detachment follows that of the anchoring case. After detachment, however, the frequency decreases rapidly,

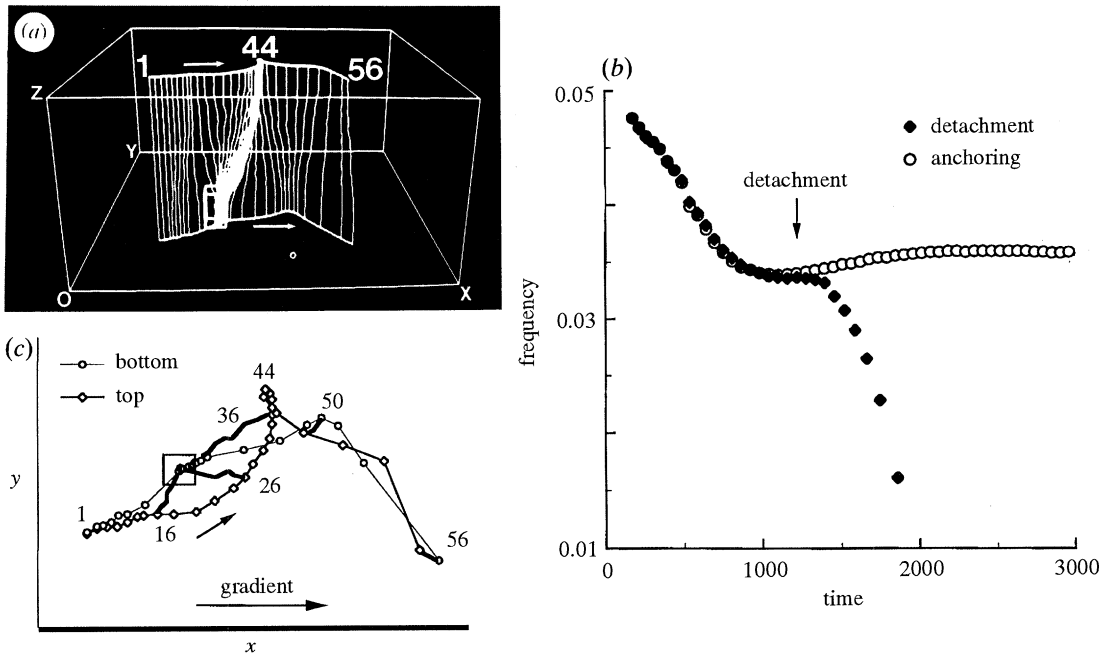

Figure 7. Detachment of a scroll wave from a localized defect. (*a*) Successive snapshots of the filament during anchoring and detachment (detachment occurs at rotation number 44). All parameters are identical to figure 6, except the defect has a slightly smaller height. (*b*) Rotation frequency versus time for anchoring and detachment. (*c*) (x, y) projection of the top and bottom of the filament during anchoring and detachment. The full filament is shown for rotations 1, 16, 26, 36, 50, and 56 (thick lines). The top of the filament curls up (rotations 1 through 44) and approaches equilibrium, until the bottom pulls free of the obstacle (at rotation 40), after which the filament executes a complicated, rotary motion. (Adapted from Vinson *et al.* 1993.)

paralleling the rotation frequency of the filament in the absence of an defect. The smaller the height of the defect, the shorter the time of temporary attachment, and thus the shorter the lifetime of the scroll wave.

(*c*) *Mechanism of anchoring and detachment*

The complex motion of the filament during anchoring and detachment can be explained by analysis of intrinsic filament motion due to deviations from a rectilinear shape (Vinson *et al.* 1993). As is well known (Keener & Tyson 1992; Panfilov *et al.* 1989), deformation of the filament causes it to move, even in a homogeneous medium; this motion is determined by local curvature, torsion, and twist (Keener & Tyson 1992). The motion of the filament during anchoring and detachment is a combination of the effects of drift and deformation of the filament as it evolves in the heterogeneous medium.

The dynamics of the filament during anchoring and detachment are consequences of the S-shaped deformation of the filament, which it acquires during the initial stages of anchoring, and retains throughout the anchoring and detachment processes (Vinson *et al.* 1993). This S-shaped deformation is a result of two effects: the zero-flux boundary condition on the free and anchored ends, which requires them to be perpendicular to the boundary of the medium, and the continued drift of the unanchored end of the filament. Once deformed from a straight-line, the

filament evolves through a combination of the effects of intrinsic motion and the extrinsic effects of the inhomogeneities. This approach accounts for the critical height, below which the filament detaches: when the height is smaller, the curvature at the defect is larger and the intrinsic motion of the filament is sufficient to detach the filament. When the effects of the local curvature-driven intrinsic motion of the filament (Keener & Tyson 1992) are combined additively with the motion due to the gradient, the complicated motion of the filament during anchoring and detachment can be explained (Vinson *et al.* 1993).

4. Conclusion

The study of dynamics in inhomogeneous media is motivated by a need to understand the behavior of vortices in real experiments, which are generally inhomogeneous, even though the dynamics of scroll waves even in homogeneous media are not fully understood. In some excitable media, such as the BZ reaction, the inhomogeneity may eventually be eliminated by improving experimental technique. In many media, however, the inhomogeneities are inherent in the system (e.g. the myocardium), and indeed are responsible for many aspects of the dynamics that have practical importance. For example, the phenomena of anchoring and detachment are important in the evolution of dangerous cardiac arrhythmias. In particular, if an arrhythmia-causing scroll wave drifts to the boundary of the myocardium, it may annihilate, leading to termination of the arrhythmia. However, if the scroll wave is anchored to a defect (such as a blood vessel or an infarcted area) then the arrhythmia may be sustained, and may require medical intervention to be terminated.

In this paper, we have summarized what is known about evolution of vortex-like patterns in three-dimensional inhomogeneous excitable media. We have shown that a smooth gradient can result in drift of the scroll (when the gradient is perpendicular to the scroll wave filament), and in twist (when the gradient is parallel to the filament). A localized defect can anchor a scroll wave drifting in a parameter gradient. The timescale for equilibration during anchoring is much longer than in two dimensions, and the scroll becomes twisted. Moreover, in three dimensions, anchoring may be temporary if the defect is below a critical size. The evolution of scroll waves in the presence of these inhomogeneities can be qualitatively understood in terms of the effects of the gradient and the intrinsic motion of the filament due to deformation.

The present status of three-dimensional studies of inhomogeneous excitable media has several limitations. So far, only the evolution of scroll waves with initially straight-line filament in inhomogeneous media have been considered. In addition, only very simple topologies of the inhomogeneity (linear gradient and isolated defect), with parallel and perpendicular orientation between the gradient and the filament, have been studied.

Another limitation is that the consideration of evolution in an inhomogeneous medium has been separated from the consideration of the initiation of scroll waves. In this review we have focused only on the evolution of scroll waves imposed by the initial condition, without considering other mechanisms of initiation. In reality, the initiation of vortices and their evolution are not independent. Certain inhomogeneities cause the production of vortices, which then evolve in the

PHILOSOPHICAL TRANSACTIONS OF THE ROYAL SOCIETY A MATHEMATICAL, PHYSICAL & ENGINEERING SCIENCES

presence of that inhomogeneity (Panfilov & Vasiev 1991). For example, a region of high refractory period may produce scroll waves, which then follow the boundary of that region (Medvinsky *et al.* 1984).

We emphasize that the cases studied thus far are extremely simple. However, this is just the first step in understanding the extremely complex motion of vortices with complicated filaments in the presence of more general topologies of the inhomogeneity.

Appendix A. Models and parameters used in numerical simulations

In this appendix we give some details of the model and parameters used in the numerical simulations described in the paper. Referring to equations (1.2) and (1.3), the function $f(E)$ is defined to be the piecewise linear function given by

$$f(E) = \begin{cases} -C_1 E & \text{for} \quad E < E_1, \\ C_2(E-a) & \text{for} \quad E_1 \leqslant E \leqslant E_2, \\ -C_3(E-1) & \text{for} \quad E > E_2. \end{cases}$$

The function $\tau(E)$ is defined (except at points within a localized inhomogeneity) to be a piecewise constant function:

$$\tau(E) = \begin{cases} \tau_1 & \text{for} \quad E < B_1, \\ \tau_2 & \text{for} \quad B_1 \leqslant E \leqslant B_2, \\ \tau_3 & \text{for} \quad E > B_2. \end{cases}$$

Within a localized inhomogeneity, τ is chosen to be a constant, $\tau_1 = \tau_2 = \tau_3 = \tau_{\text{defect}}$.

The parameter values for the functions defined above used in this paper are as follows: $C_1 = 4.0$, $C_2 = 0.9$, $C_3 = 15.0$, $E_1 = 0.018$, $\tau_1 = \tau_3 = 0.5$, $\tau_2 = 16.66$, $B_1 = 0.01$, $B_2 = 0.95$, and $\tau_{\text{defect}} = 4.0$. The parameters E_2 and a are determined by demanding continuity of the function $f(E)$: $E_2 = ((C_1+C_2)E_1+C_3)/(C_3+C_2)$, $a = E_1(C_1 + C_2)/C_2$. Similar parameters have been used elsewhere (Pertsov *et al.* 1993*a*). For the parameter of the linear gradient of equation (1.2) we use $\alpha = 0.0017$.

Equations (1.2) and (1.3) are integrated numerically using an explicit Euler integration scheme, which has been found to be stable for a range of parameter values. In the work reported here, we use time and space steps of $h_t = 0.05$ and $h_x = 0.625$. The three-dimensional calculations were carried out on the Connection Machine (CM-2) and DECmpp 2000 at the Northeast Parallel Architectures Center.

This work was supported in part by grants HL39707 and HL29439 from the National Heart and Blood Institute and Grant-in-Aid from the American Heart Association, and was conducted using the computational resources of the Northeast Parallel Architectures Center (NPAC) at Syracuse University.

References

Agladze, K. I. & de Kepper, P. 1992 BZ-waves, s propagation along a line of diffusion-jump. In *Spatio-temporal organization in nonequilibrium systems* (ed. S. C. Müller, & T. Plesser), pp. Dortmund: Projekt Verlag.

Aliev, R. & Rovinsky, A. B. 1992 Spiral waves in the homogeneous and inhomogeneous BZ reaction. *J. Phys. Chem.* **96**, 732–736.

Biktashev, V. N. 1989 Evolution of twist of an autowave vortex. *Physica* D **36**, 167–172.

Braune, M. & Engel, H. 1992 Spiral drift in a light-sensitive active medium with spatial gradient excitability. In *Spatio-temporal organization in nonequilibrium systems* (ed. S. C. Müller, & T. Plesser). Dortmund: Projekt Verlag.

Davidenko, J. M., Pertsov, A. M., Salomonsz, R., Baxter, W. & Jalife, J. 1992 Stationary and drifting spiral waves of excitation in isolated cardiac muscle. *Nature, Lond.* **335**, 349–351.

Fast, V. G. & Pertsov, A. M. 1992 Shift and termination of functional reentry in isolated ventricular preparations with quinine-induced inhomogeneity in refractory period. *J. Cardiovasc. Electrophysiol.* **3**, 255–265.

Gerisch, G. 1965 Standienpezifische Aggregationsmuster bei Distyostelium Discoideum. *Wilhelm Roux Archiv. Entwick Org.* **156**, 127–144.

Gorelova, N. A. & Bures, J. 1983 Spiral waves of spreading depression in the isolated chicken retina. *Neurobiology* **14**, 353–363.

Henze, C, Lugosi, E. & Winfree, A. T. 1990 Helical organizing centres in excitable media. *Can. J. Phys.* **68**, 683–710.

Jahnke, W., Henze, C. & Winfree, A. 1988 Chemical vortex dynamics in three-dimensional excitable media. *Nature, Lond.* **336**, 662–665.

Keener, J. P. & Tyson, J. J. 1992 The dynamics of scroll waves in excitable media. *SIAM Rev.* **34**, 1–39.

Krinsky, V. I. (ed.) 1984 *Self-organization: autowaves and structures far from equilibrium.* Berlin: Springer-Verlag.

Lechleiter, J., Girard, S., Peralta, E. & Clapham, D. 1991 Spiral calcium wave propagation and annihilation in *Xenopus laevis* oocytes. *Science, Wash.* **252**, 123–126.

Liu, D.-W., Gintant, G. A. & Antzelevitch, C. 1993 Ionic bases for electrophysiological distinctions among epicardial, midmyocardial, and endocardial myocytes from the free wall of the canine left ventricle. *Circulation Res.* **72**, 671–687.

Medvinsky, A. B., Panfilov, A. V. & Pertsov, A. M. 1984 Properties of rotating waves in three dimensions: scroll rings in myocard. In *Self-organization: autowaves and structures far from equilibrium* (ed. V. I. Krinsky), pp. 195–199. Berlin: Springer-Verlag.

Mikhailov, A. S., Panfilov, A. V. & Rudenko, A. N. 1985 Twisted scroll waves in active three-dimensional media. *Phys. Lett.* A **109**, 246–249.

Nettesheim, S., von Oertzen, A., Rotermund, H. H. & Ertl, G. 1992 Reaction diffusion patterns in the catalytic CO oxidation on Pt(110) – front propagation and spiral waves. In *Spatio-temporal organization in nonequilibrium systems* (ed. S. C. Müller & T. Plesser). Dortmund: Projekt Verlag.

Panfilov, A. V., Rudenko, A. N. & Pertsov, A. M. 1984 Twisted scroll waves in three-dimensional active media. In *self-organization: autowaves and structures far from equilibrium* (ed. V. I. Krinsky), pp. 103–105. Berlin: Springer-Verlag.

Panfilov, A. V. & Pertsov, A. M. 1984 Vortex rings in a three-dimensional medium described by reaction-diffusion equations. *Dokl. Biophys.* **274**, 58–60.

Panfilov, A. V., Aliev, R. R. & Mushinsky, A. V. 1989 An integral invariant for scroll rings in a reaction-diffusion system. *Physica* D **36**, 181–188.

Panfilov, A. V. & Vasiev, B. N. 1991 Vortex initiation in a heterogeneous excitable medium. *Physica* D **49**, 107–113.

Pertsov, A. M. & Ermakova, E. A. 1988 Mechanism of the drift of spiral wave in an inhomogeneous medium. *Biophys.* **33**, 338–341.

Pertsov, A. M., Aliev, R. R. & Krinsky, V. I. 1990 Three-dimensional twisted vortices in an excitable chemical medium. *Nature, Lond.* **345**, 419–421.

Pertsov, A. M., Davidenko, J. M., Salomonsz, R., Baxter, W. T. & Jalife, J. 1993*a* Spiral waves of excitation underlie reentrant activity in isolated cardiac muscle. *Circulation Res.* **72**, 631–650.

PHILOSOPHICAL TRANSACTIONS OF THE ROYAL SOCIETY A MATHEMATICAL, PHYSICAL & ENGINEERING SCIENCES

Pertsov, A. M., Vinson, M. & Müller, S. C. 1993*b* Three-dimensional reconstruction of organizing centers in excitable chemical media. *Physica* D **63**, 233–235.

Rudenko, A. N. & Panfilov, A. V. 1983 Drift and interaction of vortices in two-dimensional heterogeneous active medium. *Studia Biophysica* **98**, 183–188.

Schütze, J., Steinbock, O. & Müller, S. C. 1992 Forced vortex interaction and annihilation in an active medium. *Nature, Lond.* **356**, 45–47.

Siegert, F. & Weijer, C. 1991 Analysis of optical density wave propagation and cell movement in the cellular slime mold *Dictyostelium discoideum*. *Physica* D **49**, 224–232.

Siegert, F., Steinbock, O., Weijer, C. J. & Müller, S. C. 1992 Three-dimensional autowaves control cell motion in Dictyostelium slugs. In *Spatio-temporal organization in nonequilibrium systems* (ed. S. C. Müller & T. Plesser). Dortmund: Projekt Verlag.

Skinner, G. S. & Swinney, H. L. 1991 Periodic to quasiperiodic transition of chemical spiral waves. *Physica* D **48**, 1–16.

Steinbock, O., Schütze, J. & Müller, S. C. 1992 Electric-field-induced drift and deformation of spiral waves in an excitable medium. *Phys. Rev. Lett.* **68**, 248–251.

Swinney, H. L. & Krinsky, V. I. (eds) 1991 Waves and patterns in chemical and biological media. *Physica* D **49**.

Vinson, M., Pertsov, A. M. & Jalife, J. 1993 Anchoring of vortex filaments in 3D excitable media. *Physica* D **72**, 119–134.

Welsh, B., Gomatam, S. & Burgess, A. 1983 Three-dimensional chemical waves in the Belousov–Zhabotinsky reaction. *Nature, Lond.* **304**, 611–614.

Winfree, A. T. 1972 Spiral waves of chemical activity. *Science, Wash.* **175**, 634–636.

Winfree, A. T. 1973 Scroll-shaped waves of chemical activity in three dimensions. *Science, Wash.* **181**, 937–939.

Winfree, A. T. & Strogatz, S. H. 1984 Organizing centers for three-dimensional chemical waves. *Nature, Lond.* **311**, 611–615.

Winfree, A. T. 1990 Stable particle-like solutions to the nonlinear wave equations of three-dimensional excitable media. *SIAM Rev.* **32**, 1–53.

Yamaguchi, T. & Müller, S. C. 1991 Front geometries of chemical waves under anisotropic conditions. *Physica* D **49**, 40–46.

Zhabotinsky, A. M. & Zaikin, A. N. 1971 *Oscillatory processes in biological and chemical systems*, vol. 2, pp. 279–283. Pushchino: on Oka.

Zou, X., Levine, H. & Kessler, D. A. 1993 Interaction between a drifting spiral and defects. *Phys. Rev.* E**47**, R800–R803.

PHILOSOPHICAL TRANSACTIONS OF THE ROYAL SOCIETY A MATHEMATICAL, PHYSICAL & ENGINEERING SCIENCES

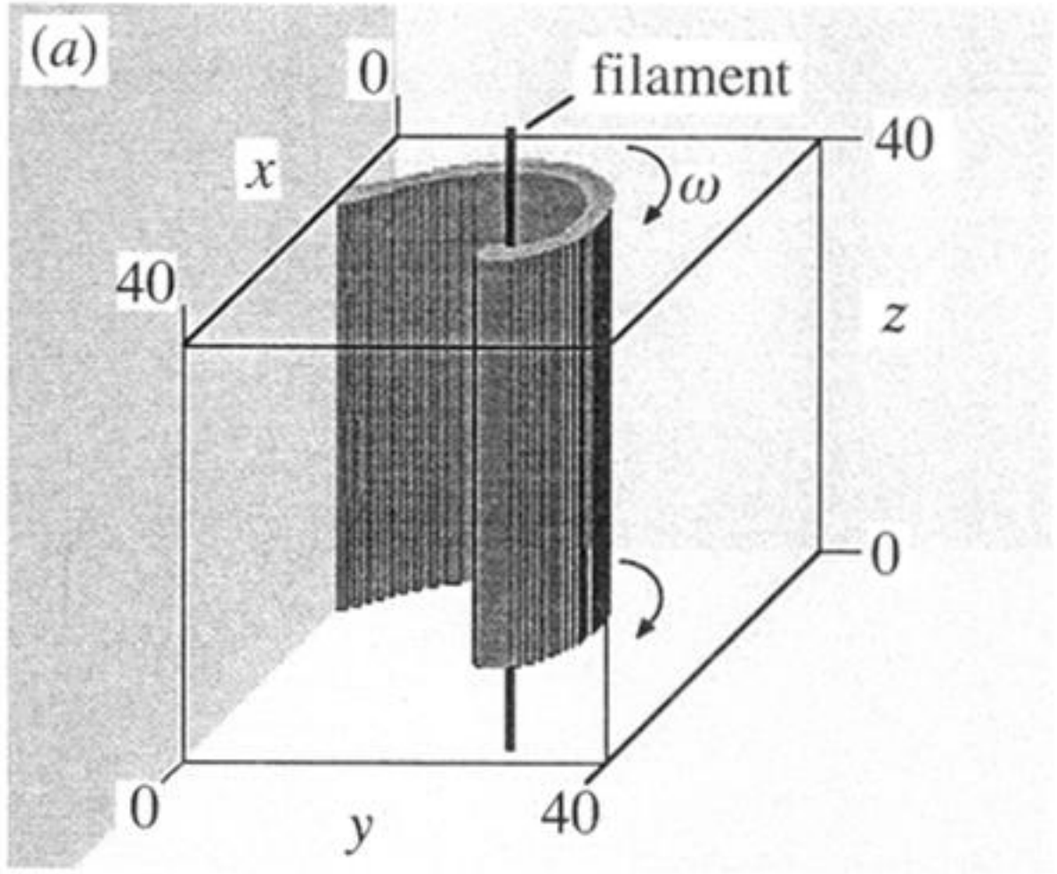

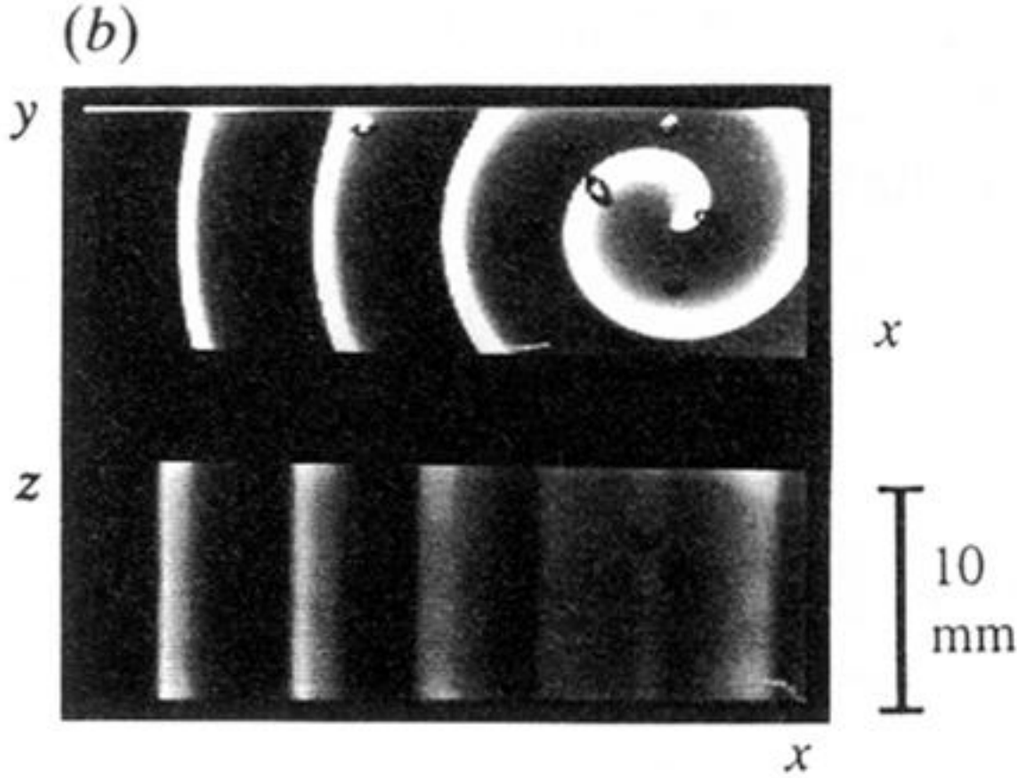

igure 1. Scroll wave with straight-line filament. (*a*) From the computer simulation of itzHugh–Nagumo model. The activated (excited) regions are shown in dark gray. The fila- ent is the phase singularity around which the scroll rotates, shown as a heavy dark line. rrows show the direction of rotation of the scroll; the scroll rotates with angular frequency ω.) Two projections of a scroll wave in BZ reaction. In the (x, y) projection, the scroll appears s a spiral; in the (x, z) projection, the wave appears as a set of planar waves.

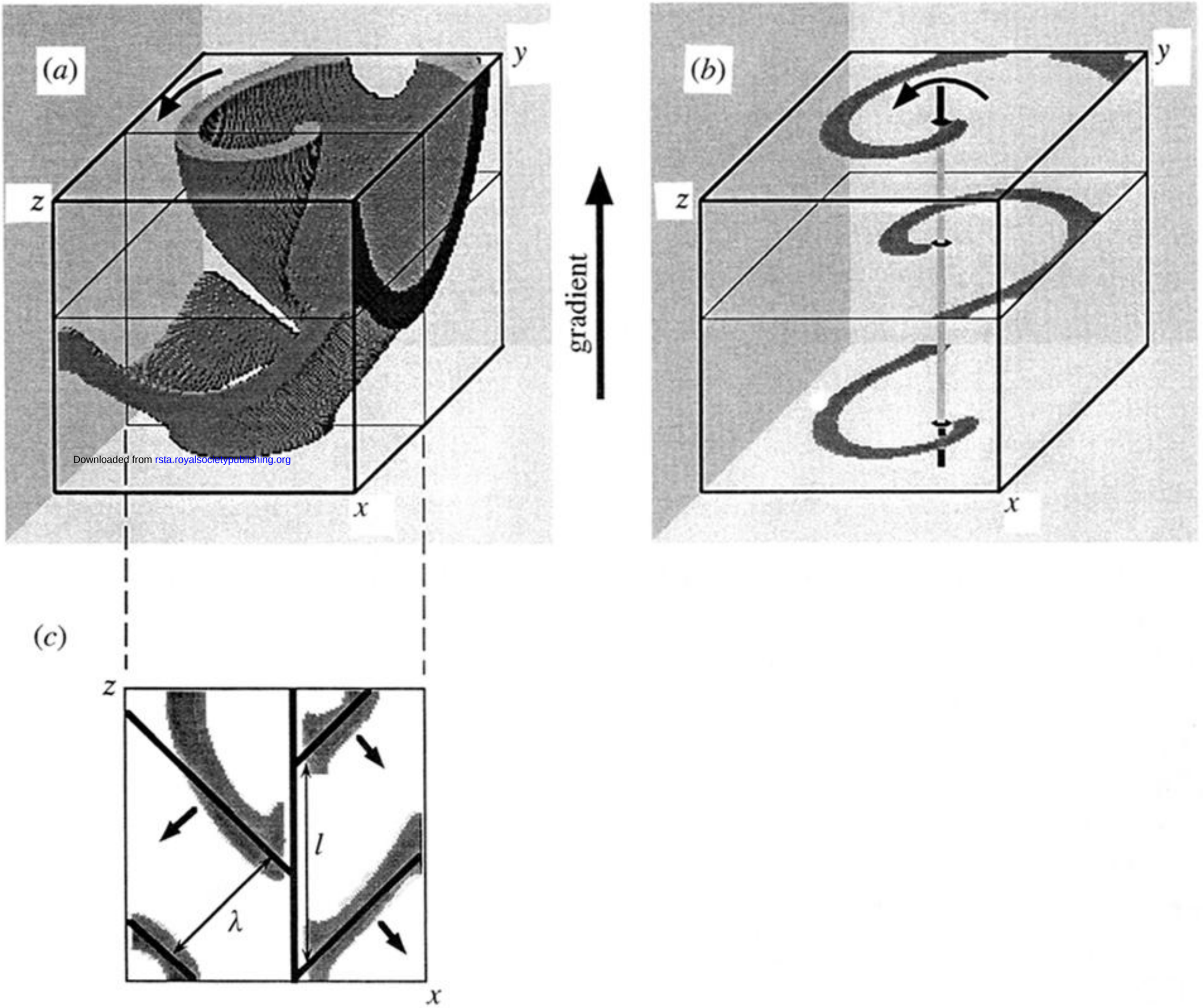

Figure 4. Twisted scroll wave in parameter gradient parallel to the filament. (*a*) Equilibrium twisted scroll from FitzHugh–Nagumo computer simulation. The conic structure is typical of a twisted scroll. (*b*) Three horizontal cross sections of the scroll in part (*a*), showing the spiral structure. The filament is shown as a gray line. (*c*) A vertical cross section of the twisted scroll through the filament, demonstrating the specific branching structure indicative of twist. Arrows show the direction of propagation. The central vertical line is the filament, the branching lines follow the wave fronts. λ is the wavelength of the scroll, and ℓ is the distance over which the phase shift is 2π. The twist is then $w = 2\pi/\ell$.

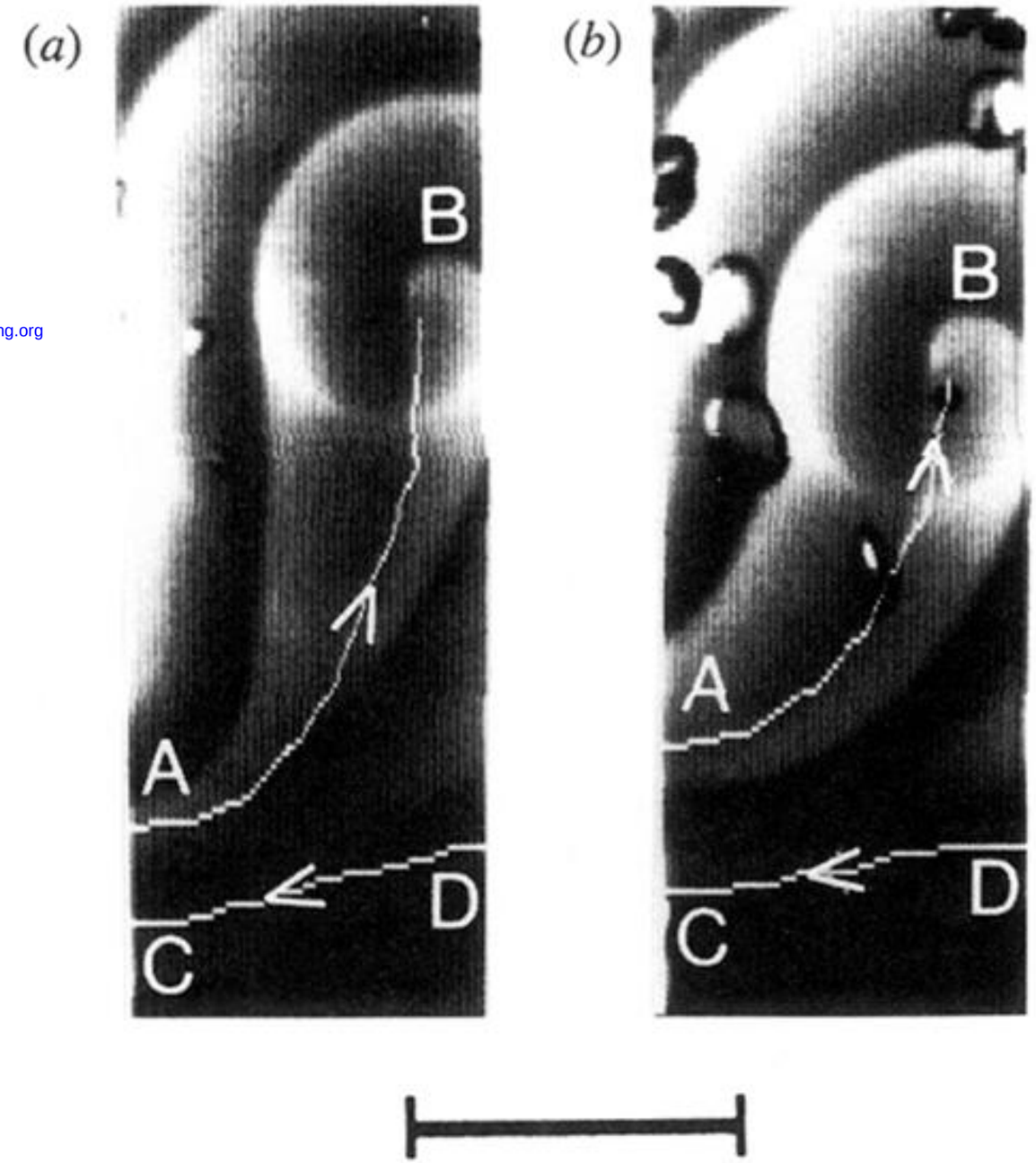

Figure 5. Snapshots of twisted scroll waves from BZ reaction experiment. Front view. The white lines show the positions of the filaments, with arrows indicating sense of rotation. (*a*) Scroll waves shortly after initiation. Filament A-B is significantly twisted, as can be seen from the characteristic conical shape of the wave front (compare figure 4). The twist is due to a temperature gradient in the vertical direction. Horizontally oriented filament C-D is less twisted because its projection in the direction of the gradient is small. (*b*) The same scroll waves one hour later (30 min after removal of gradient). The filaments became shorter and show a smaller degree of twist. Figure from Pertsov *et al.* (unpublished data).

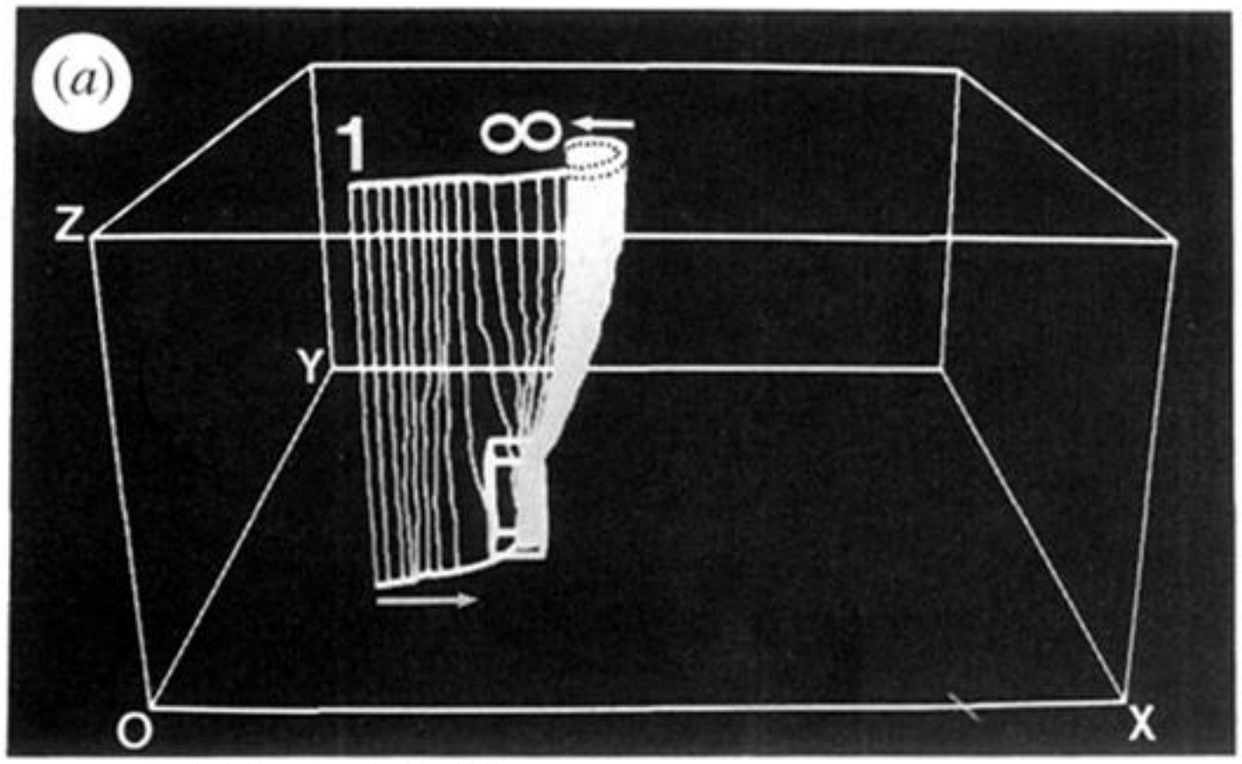

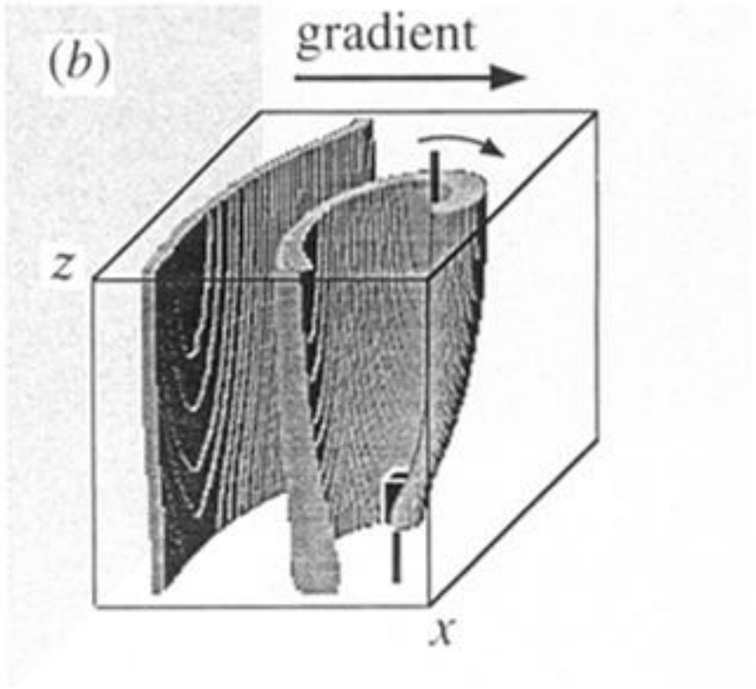

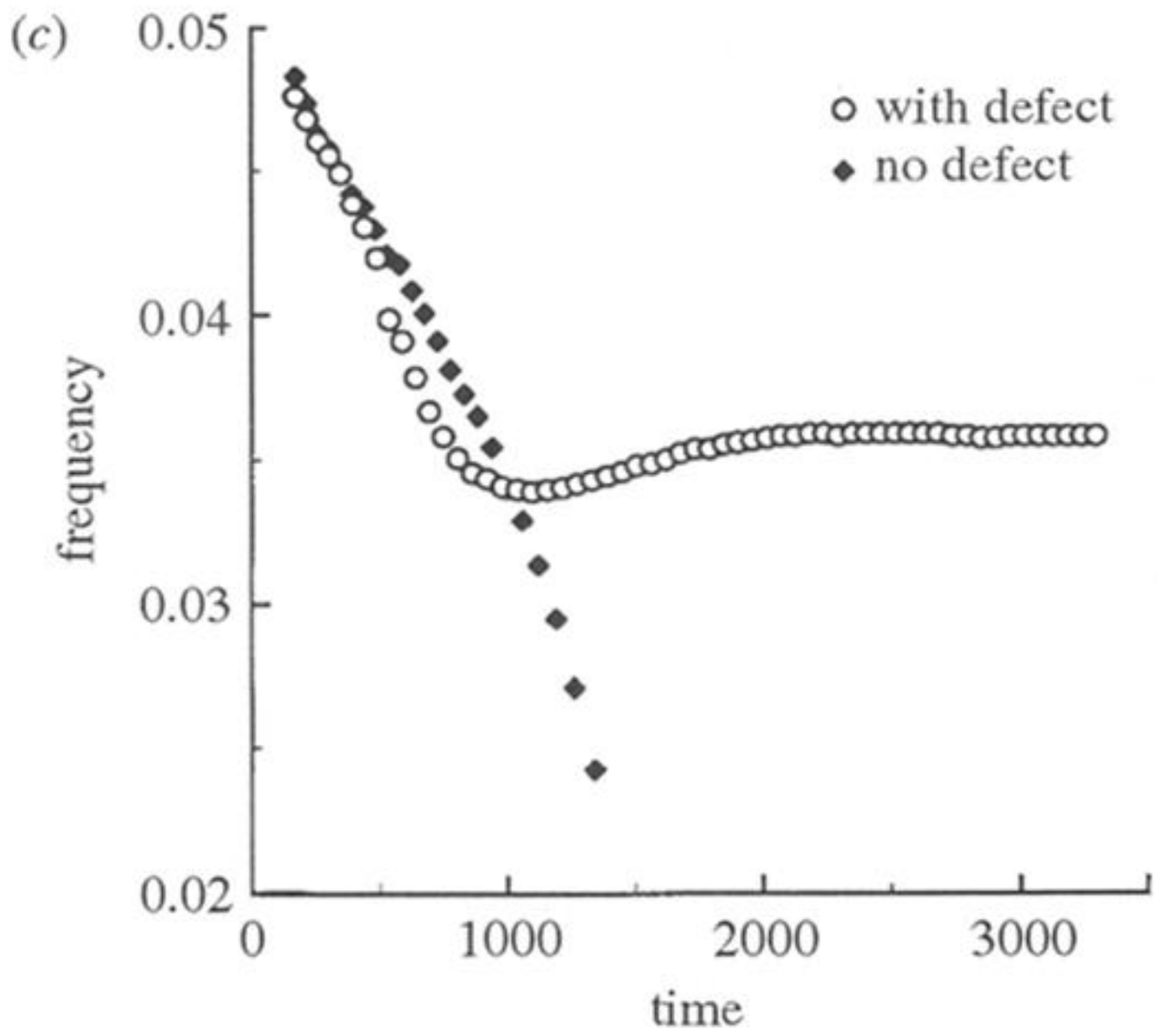

Figure 6. Anchoring of a scroll wave to a localized defect. (*a*) Successive snapshots of the filament during the anchoring process. The parameter gradient is to the right ($+x$ direction). Parameters as in figure 2, with the addition of a localized defect. (*b*) Snapshot of anchored scroll wave. The effect of twist can be seen in the conic shape of the wave front (cf. figure 4). (*c*) Rotation frequency versus time with and without the defect. (Adapted from Vinson *et al.* 1993.)